Reactions of (η^6:η^1-$C_6H_5CH_2CH_2PR_2$)$Ru(CH_3)_2$ (R = Cy, Ph) with $[H(Et_2O)_2][B(3,5\text{-}C_6H_3(CF_3)_2)_4]$ in the Presence of Carbon Monoxide, Acetylene, Ethylene, and Norbornene

Kayo Umezawa-Vizzini and T. Randall Lee*

Department of Chemistry, University of Houston, 4800 Calhoun Road, Houston, Texas 77204-5003

Received January 7, 2003

The reactions of (η^6:η^1-$C_6H_5CH_2CH_2PR_2$)$Ru(CH_3)_2$, where R = Cy (**1**), Ph (**2**), with boron activators in the presence of CO, acetylene, ethylene, and norbornene were explored. The reaction of **1** and **2** with $H(Et_2O)_2[B(3,5\text{-}C_6H_3(CF_3)_2)_4]$ ($\mathbf{H^+B^-}$) in the presence of CO afforded [(η^6:η^1-$C_6H_5CH_2CH_2PR_2$)$Ru(CH_3)(CO)$][$B(3,5\text{-}C_6H_3(CF_3)_2)_4$] (**3** and **4**, respectively). The reaction of **1** and **2** with $\mathbf{H^+B^-}$ in the presence of acetylene afforded polyacetylene and [(η^6-$C_6H_5CH_2CH_2PR_2$)Ru(η^3-$CH_3CHC_5H_5$)][$B(3,5\text{-}C_6H_3(CF_3)_2)_4$] (**5** and **6**, respectively). The latter reactions were proposed to proceed via coordinative insertion of acetylene into Ru−alkyl bonds. In contrast, the reaction of **2** with $\mathbf{H^+B^-}$ in the presence of ethylene initially afforded the precursor complex [(η^6:η^1-$C_6H_5CH_2CH_2PPh_2$)$Ru-CH_3(CH_2{=}CH_2)$]$_2$[$B(3,5\text{-}C_6H_3(CF_3)_2)_4$]$_2$, which decomposed to give the dimeric species [(η^6:η^1-$C_6H_5CH_2CH_2PPh_2$)RuCl][$B(3,5\text{-}C_6H_3(CF_3)_2)_4$] (**7**). Finally, the reaction of **1** and **2** with $\mathbf{H^+B^-}$ in the presence of excess norbornene afforded ring-opened polynorbornene, presumably via Ru-catalyzed ring-opening metathesis polymerization (ROMP). The reaction products were characterized by IR and NMR spectroscopy. Single-crystal X-ray structural analyses of complexes **3**, **5**, **6**, and **7** were also performed.

Introduction

The insertion of unsaturated organic species such as alkenes, alkynes, conjugated dienes, and carbon monoxide into metal−carbon bonds is perhaps the most critical step in oligomerization and polymerization reactions. This step exhibits at least four distinct flavors: (1) coordinative insertion of an unsaturated bond into a metal−alkyl bond,[1−4] (2) π-bond metathesis involving metal−carbene complexes,[5−10] (3) oxidative coupling of alkynes,[11,12] and (4) insertion of metal−allyl bonds.[13,14] Coordinative insertion chemistry has been widely utilized in industry to generate polymeric materials and lubricants from the inexpensive byproducts of petroleum cracking. Traditionally, the catalytic polymerization of olefins has utilized early transition metals, namely those in groups IV and V.[1−3] Recently, however, polymerization catalysts have been developed using transition metals from groups VIII−X (e.g., Fe,[15−20] Co,[15−18] Rh,[21] Ni,[22−28] and Pd[23,24,26]) because the less oxophilic nature of the late transition metals holds promise for the

* To whom correspondence should be addressed. E-mail: trlee@uh.edu.

(1) For example, see: Boor, J. *Ziegler−Natta Catalysts and Polymerizations*; Academic: New York, 1979.
(2) Coates, G. W.; Waymouth, R. M. In *Comprehensive Organometallic Chemistry II*; Abel, E. W., Stone, F. G. A., Wilkinson, G., Eds.; Hegedus, L., Vol. Ed.; Pergamon: New York, 1995; Vol. 12, p 1193.
(3) Brintzinger, H.; Fischer, D.; Mulhaupt, R.; Rieger, B.; Waymouth, R. *Angew. Chem., Int. Ed. Engl.* **1995**, *34*, 1143.
(4) Collman, J. P.; Hegedus, L. S.; Norton, J. R.; Finke, R. G. *Principles and Applications of Organotransition Metal Chemistry*; University Science: Mill Valley, CA, 1987.
(5) Grubbs, R. H.; Tumas, W. *Science* **1989**, *243*, 907.
(6) Grubbs, R. H. In *Comprehensive Organometallic Chemistry I*; Wilkinson, G., Ed.; Pergamon: New York, 1982; Vol. 8, p 499.
(7) Maughon, B. R.; Grubbs, R. H. *Macromolecules* **1997**, *30*, 3459.
(8) Hillmyer, M. A.; Gutierrez, E.; Grubbs, R. H. *Macromolecules* **1995**, *28*, 7256.
(9) Scherman, O. A.; Kim, H. M.; Grubbs, R. H. *Macromolecules* **2002**, *35*, 5366.
(10) Saive, E.; Demonceau, A.; Noels, A. F. *Chem. Commun.* **1995**, 1127.
(11) Vollhardt, K. P. C. *Angew. Chem., Int. Ed. Engl.* **1984**, *23*, 539.
(12) Schore, N. E. *Chem. Rev.* **1988**, *88*, 1081.
(13) Jolly, P. W. In *Comprehensive Organometallic Chemistry I*; Wilkinson, G., Stone, F. G. A., Abel, E. W., Eds.; Pergamon: New York, 1982; Vol. 8, p 671.
(14) Wilke, G. *Angew. Chem., Int. Ed. Engl.* **1963**, *2*, 105.
(15) Small, B. L.; Brookhart, M.; Bennett, A. M. *J. Am. Chem. Soc.* **1998**, *120*, 4049.
(16) Britovsek, G. J. P.; Gibson, V. C.; Kimberley, B. S.; Maddox, P. J.; McTavish, S. J.; Solan, G. A.; White, A. J. P.; Williams, D. J. *Chem. Commun.* **1998**, 849.
(17) Britovsek, G. J. P.; Bruce, M.; Gibson, V. C.; Kimberley, B. S.; Maddox, P. J.; Mastroianni, S.; McTavish, S. J.; Redshaw, C.; Solan, G. A.; Strömberg, S.; White, A. J. P.; Williams, D. J. *J. Am. Chem. Soc.* **1999**, *121*, 8728.
(18) Britovsek, G. J. P.; Gibson, V. C.; Spitzmesser, S. K.; Tellmann, K. P.; White, A. J. P.; Williams, D. J. *J. Chem. Soc., Dalton Trans.* **2002**, *6*, 1159.
(19) Brooke, L.; Brookhart, M. *Macromolecules* **1999**, *32*, 2120.
(20) Pellecchia, C.; Mazzeo, M.; Pappalardo, D. *Macromol. Rapid Commun.* **1998**, *19*, 615.
(21) Wang, L.; Lu, R. S.; Bau, R.; Flood, T. C. *J. Am. Chem. Soc.* **1993**, *115*, 6999.
(22) Younkin, T. R.; Connor, E. F.; Henderson, J. I.; Friedrich, S. K.; Grubbs, R. H.; Bansleben, D. A. *Science* **2000**, *287*, 460.
(23) Johnson, L. K.; Killian, C. M.; Brookhart, M. *J. Am. Chem. Soc.* **1995**, *117*, 6414.
(24) Killian, C. M.; Tempel, D. J.; Johnson, L. K.; Brookhart, M. *J. Am. Chem. Soc.* **1996**, *118*, 11664.
(25) Conner, E. F.; Younkin, T. R.; Henderson, J. I.; Hwang, S.; Grubbs, R. H.; Roberts, W. P.; Litzau, J. *J. Polym. Sci., Part A* **2002**, *40*, 2842.
(26) Mecking, S.; Johnson, L. K.; Wang, L.; Brookhart, M. *J. Am. Chem. Soc.* **1998**, *120*, 888.
(27) Preishuber-Pflugl, P.; Brookhart, M. *Macromolecules* **2002**, *35*, 6074.

10.1021/om030008s CCC: $25.00
Publication on Web 06/18/2003

polymerization of olefins containing polar functional groups.[26,29] Furthermore, the unique isomerization chemistry exhibited by these metals offers control over chain branching by simply varying the temperature and/or pressure.[23]

A variety of metals, including those in groups IV, V, and VIII, catalyze carbon−carbon bond metathesis via metal carbenes.[5−10] In some cases, the catalysts have been shown to promote the living ring-opening metathesis polymerization (ROMP) of cyclic olefins.[5] Additionally, ruthenium-based catalysts have been shown to initiate the ROMP of cyclic olefins containing polar functional groups.[7−10] Despite these developments, examples of the coordinative insertion of olefins into ruthenium−carbon bonds are remarkably limited.[30−33] To this end, our research has been targeting the development of ruthenium-based coordinative insertion polymerization catalysts that can tolerate alkene monomers functionalized with polar moieties.[34−37]

In this paper, we examine the reactions of (η^6:η^1-$C_6H_5CH_2CH_2PR_2$)$Ru(CH_3)_2$ (R = Cy (**1**), Ph (**2**)) with $[H(Et_2O)_2][B(3,5\text{-}C_6H_3(CF_3)_2)_4]$ (**H**$^+$**B**$^-$) in the presence of CO, acetylene, ethylene, and norbornene. In the presence of CO, the reaction of complexes **1** and **2** with **H**$^+$**B**$^-$ led to the generation of the complexes [(η^6:η^1-$C_6H_5CH_2CH_2PR_2$)$RuCH_3CO$][$B(3,5\text{-}C_6H_3(CF_3)_2)_4$], where R = Cy (**3**), Ph (**4**), respectively. In the presence of acetylene, similar reaction with **H**$^+$**B**$^-$ afforded polyacetylene and [(η^6:η^1-$C_6H_5CH_2CH_2PR_2$)Ru(η^3-$CH_3CHC_5H_5$)][$B(3,5\text{-}C_6H_3(CF_3)_2)_4$], where R = Cy (**5**), Ph (**6**), respectively. In the presence of ethylene, reaction of **2** with **H**$^+$**B**$^-$ initially formed [(η^6:η^1-$C_6H_5CH_2CH_2PPh_2$)-$RuCH_3(CH_2{=}CH_2)$][$B(3,5\text{-}C_6H_3(CF_3)_2)_4$]; this species, however, decomposed over time, and the decomposition product, [(η^6:η^1-$C_6H_5CH_2CH_2PPh_2$)$RuCl$]$_2$[$B(3,5\text{-}C_6H_3(CF_3)_2)_4$]$_2$ (**7**), was isolated. Reaction of complexes **1** and **2** with various activating agents in the presence of excess norbornene afforded ring-opened polynorbornene. Finally, specific reaction mechanisms are proposed to rationalize the formation of the indicated products.

Results and Discussion

Reaction of 1 and 2 with H$^+$B$^-$ in the Presence of CO. Using CH_2Cl_2 as solvent, we examined the reaction of complexes **1** and **2** with **H**$^+$**B**$^-$ in the presence of CO to evaluate whether the activator abstracts a methide (CH_3^-) or a hydride (H^-) from the methyl group, as has been proposed for the reaction of Ph_3CX (X = PF_6^-, BF_4^-) with several late-transition-metal dimethyl complexes.[36,38,39] As illustrated in eq 1, the reaction of **1** and **2** with 0.9 equiv of **H**$^+$**B**$^-$ afforded **3** and **4**.[40] Compound **3** was isolated as light yellow crystals by the addition of hexane to the concentrated reaction mixture. Similar treatment of **4**, however, afforded an oil that exhibited a ^{1}H NMR spectrum consistent with its proposed structure. Crystallization of the oil from a mixture of CH_2Cl_2 and hexane afforded light yellow oil-coated crystals of **4** after 1−2 weeks at room temperature. Compounds **3** and **4** were both insoluble in hexanes and slightly soluble in benzene.

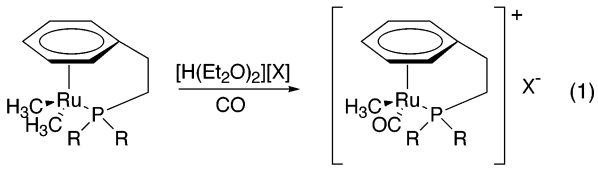

X = $B(3,5\text{-}C_6H_3(CF_3)_2)_4$; R = Cy (**3**) and Ph (**4**)

Analysis by ^{1}H NMR spectroscopy revealed Ru*C*H_3 groups at δ 0.53 (**3**) and 0.29 (**4**) as doublets with J_{PH} = 3.0 and 5.0 Hz, respectively. The chemical shifts and coupling constants are consistent with that of the reported nontethered analogue [(η^6-C_6Me_6)$RuPPh_3CH_3$-CO][BF_4], where the Ru*C*H_3 group appeared at δ 0.23 as a doublet with J_{PH} = 5.0 Hz.[41] In the ^{13}C spectra, we assign the doublets at δ −22.0 (**3**) and −16.8 (**4**), where J_{CP} = 7.6 and 7.0 Hz, respectively, to the Ru*C*H_3 carbons, and the weak resonances at δ 198 (**3**) and 196 (**4**) to the Ru*CO* carbons. The latter chemical shifts fall within the range commonly observed for the terminal carbonyl groups of metal carbonyl compounds (δ 150−220).[42] The IR spectra show coordinated CO stretching bands at 2017 (**3**) and 2004 cm^{-1} (**4**).[42]

The corresponding thermal ellipsoid plot of **3** and a view perpendicular to the η^6-phenyl moiety are shown in Figure 1; selected bond distances and angles are provided in Table 1. The bond distance of Ru−C(2) (2.150(4) Å) is similar to that of the dialkyl compound (η^6:η^1-$C_6H_5CH_2CH_2PCy_2$)$Ru(CH_3)_2$ (**1**).[36] The bond distance C(1)−O(1) is 1.135(5) Å, and the bond angle Ru−C(1)−O(1) is 178.4(4)°, which are typical values for terminal metal carbonyl groups.[4] The slight increase in the C−O bond distance relative to that for free carbon monoxide (1.128 Å) is probably due to π back-bonding.[4] The three ligands (CH_3, CO, P) lie in a slightly staggered conformation relative to the coordinated arene. The bond distances from Ru to each of the coordinated arene carbons are as follows: 2.257(4) Å, Ru−C(5); 2.290(4) Å, Ru−C(6); 2.272(4) Å, Ru−C(7); 2.293(4) Å, Ru−C(8); 2.291(4) Å, Ru−C(9); 2.276(3) Å, Ru−C(10). As observed for the dialkyl compound **1**,[36] the ruthenium metal lies almost directly beneath the center of the coordinated arene. The elongated Ru−C(8) bonds and the shortened

(28) Liu, W.; Malinoski, J. M.; Brookhart, M. *Organometallics* **2002**, 21, 2836.
(29) Younkin, T. R.; Connor, E. F.; Henderson, J. I.; Friedrich, S. K.; Grubbs, R. H.; Bansleben, D. A. *Science* **2000**, *287*, 460.
(30) James, B. R.; Markham, L. D. *J. Catal.* **1972**, *27*, 442.
(31) Komita, S.; Yamamoto, A.; Ikeda, S. *Bull. Chem. Soc. Jpn.* **1975**, *48*, 101.
(32) Nomura, K.; Warit, S.; Imanishi, Y. *Macromolecules* **1999**, *32*, 4732.
(33) Nomura, K.; Warit, S.; Yukio, I. *Bull. Chem. Soc. Jpn.* **2000**, *73*, 599.
(34) Umezawa-Vizzini, K.; Lee, T. R. *Organometallics* **1997**, *16*, 5613.
(35) Umezawa-Vizzini, K.; Lee, T. R. *J. Organomet. Chem.* **1999**, *579*, 122.
(36) Umezawa-Vizzini, K.; Guzman-Jimenez, I. Y.; Whitmire, K. H.; Lee, T. R. *Organometallics* **2003**, *22*, 3059.
(37) Umezawa-Vizzini, K.; Lee, T. R. Submitted for publication in *Organometallics*.
(38) Kletzin, H.; Werner, H.; Serhadli, O.; Ziegler, M. L. *Angew. Chem., Int. Ed. Engl.* **1983**, *22*, 46.
(39) Werner, H.; Kletzin, H.; Hohn, A.; Paul, W.; Knaup, W.; Ziegler, M. L.; Serhadli, O. *J. Organomet. Chem.* **1986**, *306*, 227.
(40) In contrast to the reaction with **H**$^+$**B**$^-$, treatment of **1** and **2** with CPh_3X (X = BF_4, PF_6) in the presence of carbon monoxide produced a mixture of two complexes: [(η^6:η^1-$C_6H_5CH_2CH_2PR_2$)$RuH(CH_2{=}CH_2)$][X] and [(η^6:η^1-$C_6H_5CH_2CH_2PR_2$)$RuCH_3(CO)$][X] in a ratio of approximately 4:1, respectively, as judged by ^{1}H NMR spectroscopy.
(41) Kletzin, H.; Werner, H. *J. Organomet. Chem.* **1985**, *291*, 213.
(42) Elschenbroich, C.; Salzer, A. *Organometallics: A Concise Introduction*; VCH: New York, 1992.

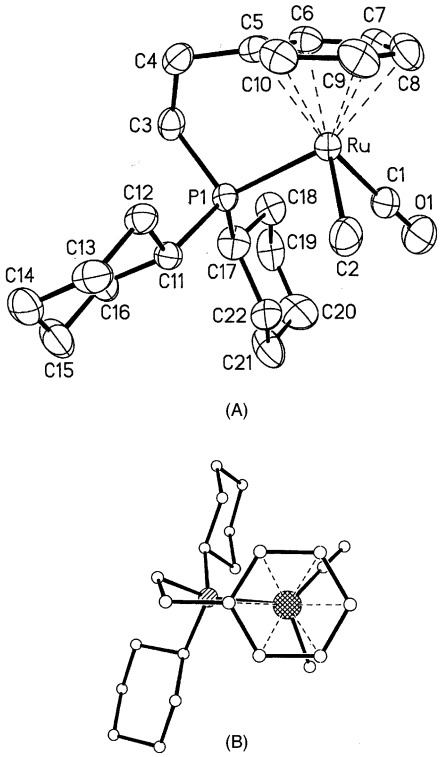

Figure 1. (A) Thermal ellipsoid plot of [(η^6:η^1-$C_6H_5CH_2$-CH_2PCy_2)$RuCH_3CO$][B(3,5-$C_6H_3(CF_3)_2$)$_4$] (**3**) at the 40% probability level and (B) a view perpendicular to the η^6 aromatic ring.

Table 1. Selected Bond Lengths (Å) and Angles (deg) for 3

Bond Lengths			
Ru−C(1)	1.874(4)	Ru−C(2)	2.150(4)
Ru−C(5)	2.257(4)	Ru−C(10)	2.276(3)
Ru−C(9)	2.291(4)	Ru−C(7)	2.272(4)
Ru−C(6)	2.290(4)	Ru−P(1)	2.3198(9)
Ru−C(8)	2.293(4)	O(1)−C(1)	1.135(5)
Bond Angles			
C(1)−Ru−C(2)	81.43(19)	C(1)−Ru−C(5)	146.87(17)
C(2)−Ru−C(5)	131.15(16)	C(1)−Ru−C(7)	94.26(16)
C(2)−Ru−C(7)	141.12(15)	C(5)−Ru−C(7)	64.86(14)
C(1)−Ru−C(10)	165.94(16)	C(2)−Ru−C(10)	99.60(17)
C(5)−Ru−C(10)	36.60(14)	C(7)−Ru−C(10)	76.06(15)
C(1)−Ru−C(6)	113.11(16)	C(2)−Ru−C(6)	163.69(16)
C(5)−Ru−C(6)	35.99(13)	C(7)−Ru−C(6)	35.54(14)
C(10)−Ru−C(6)	64.47(14)	C(1)−Ru−C(9)	130.49(17)
C(2)−Ru−C(9)	89.52(17)	C(5)−Ru−C(9)	65.22(15)
C(7)−Ru−C(9)	64.07(15)	C(10)−Ru−C(9)	35.95(15)
C(6)−Ru−C(9)	75.48(15)	C(1)−Ru−C(8)	102.06(17)
C(2)−Ru−C(8)	107.19(16)	C(5)−Ru−C(8)	76.40(15)
C(7)−Ru−C(8)	35.69(15)	C(10)−Ru−C(8)	64.14(15)
C(6)−Ru−C(8)	63.79(15)	C(9)−Ru−C(8)	35.36(16)
C(1)−Ru−P(1)	94.51(13)	C(2)−Ru−P(1)	91.08(12)
O(1)−C(1)−Ru	178.4(4)		

Ru−C(5) bonds probably arise from tilting of the coordinated arene induced by the presence of the two-carbon bridge, although the trans influence of the phosphine might also play a role.[43]

Reaction of 1 and 2 with H^+B^- in the Presence of HC≡CH. Using CH_2Cl_2 as solvent, the reaction of complexes **1** and **2** with H^+B^- in the presence of acetylene afforded polyacetylene[44] and the complexes

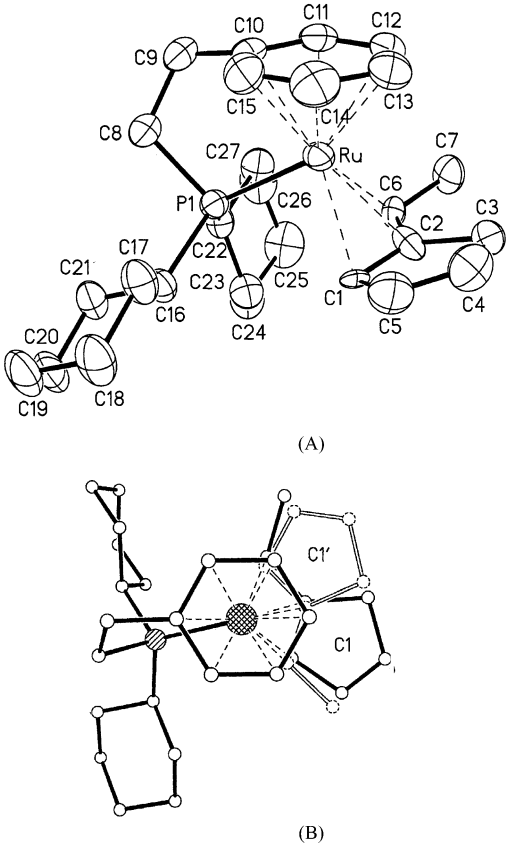

Figure 2. (A) Thermal ellipsoid plot of [(η^6:η^1-$C_6H_5CH_2$-CH_2PCy_2)Ru(η^3-$CH_3CHC_5H_5$)][B(3,5-$C_6H_3(CF_3)_2$)$_4$] (**5**) at the 40% probability level and (B) and a view perpendicular to the η^6 aromatic ring.

[(η^6:η^1-$C_6H_5CH_2CH_2PR_2$)Ru(η^3-$CH_3CHC_5H_5$)][B(3,5-C_6H_3-$(CF_3)_2$)$_4$], where R = Cy (**5**), Ph (**6**), respectively, in about 50% yield each (eq 2). While the ^{1}H NMR spectra showed the presence of clean products, we were unable

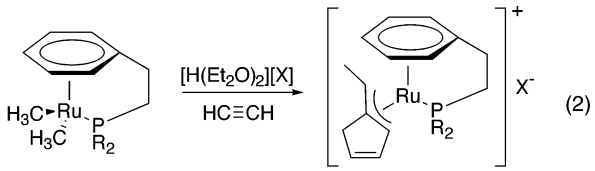

(2)

X = B(3,5-$C_6H_3(CF_3)_2$)$_4$; R = Cy (**5**) and Ph (**6**)

to isolate compounds **5** and **6** in purely crystalline or powder form; at room temperature, the compounds existed as oils that were insoluble in hexanes and slightly soluble in benzene. Upon attempted recrystallization of the oily products from a mixture of CH_2Cl_2 and *n*-hexane, reddish brown single crystals of **5** and **6** were observed to grow in the oily suspensions at room temperature. These crystals were rinsed with hexanes, and single-crystal X-ray structural analyses were performed on the oil-coated crystals of both **5** and **6**.[45] The corresponding thermal ellipsoid plots are shown in Figures 2 and 3, respectively, and selected bond distances and angles are given in Tables 2 and 3, respectively. While the allyl ligand of compound **6** exhibited an ordered structure, that of compound **5** was disordered

(43) Therrien, B.; Ward, T. R.; Pilkington, M.; Hoffmann, C.; Gilardoni, F.; Weber, J. *Organometallics* **1998**, *17*, 330.

(44) Polyacetylene was obtained as a black powder. This powder was completely consumed in a flame with no ash remaining.

(45) Before X-ray analysis, the oily coatings were partially removed from the crystals by gentle scraping with a microspatula.

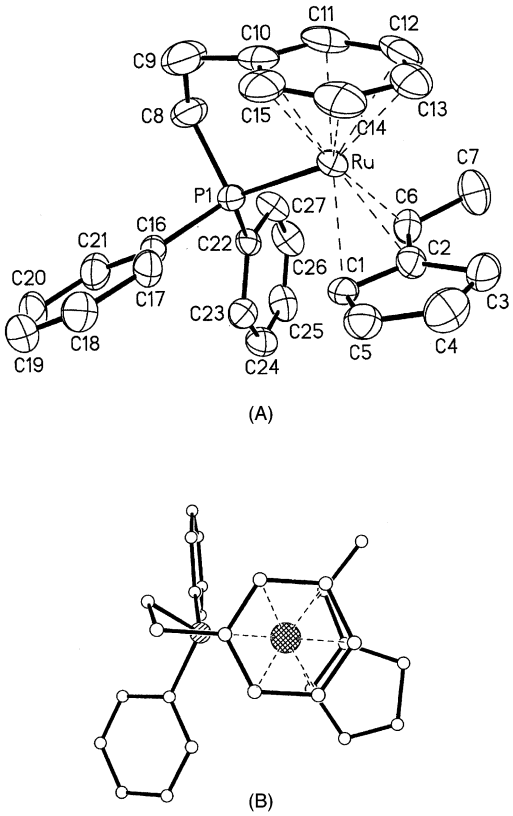

Figure 3. (A) Thermal ellipsoid plot of $[(\eta^6:\eta^1\text{-}C_6H_5CH_2\text{-}CH_2PPh_2)Ru(\eta^3\text{-}CH_3CHC_5H_5)][B(3,5\text{-}C_6H_3(CF_3)_2)_4]$ (**6**) at the 40% probability level and (B) a view perpendicular to the η^6 aromatic ring.

Table 2. Selected Bond Lengths (Å) and Angles (deg) for 5

Bond Lengths			
Ru−C(2)	2.203(7)	Ru−C(6)	2.218(6)
Ru−C(10)	2.219(3)	Ru−C(12)	2.230(3)
Ru−C(15)	2.238(3)	Ru−C(11)	2.241(3)
Ru−C(14)	2.246(4)	Ru−P(1)	2.3622(8)
Ru−C(13)	2.257(4)	Ru−C(1)	2.313(6)
C(1)−C(2)	1.414(6)	C(2)−C(6)	1.404(6)

Bond Angles			
C(6)−Ru−C(2)	37.02(17)	C(2)−Ru−C(10)	167.18(17)
C(6)−Ru−C(10)	134.98(17)	C(2)−Ru−C(12)	101.70(18)
C(6)−Ru−C(12)	93.19(19)	C(10)−Ru−C(12)	66.48(13)
C(6)−Ru−C(15)	169.62(19)	C(2)−Ru−C(15)	149.06(18)
C(10)−Ru−C(15)	36.65(14)	C(12)−Ru−C(15)	77.55(14)
C(2)−Ru−C(11)	130.37(17)	C(6)−Ru−C(11)	104.15(18)
C(10)−Ru−C(11)	36.85(12)	C(12)−Ru−C(11)	36.74(14)
C(15)−Ru−C(11)	65.61(14)	C(2)−Ru−C(14)	114.79(18)
C(6)−Ru−C(14)	142.98(18)	C(10)−Ru−C(14)	65.98(15)
C(12)−Ru−C(14)	65.67(16)	C(15)−Ru−C(14)	36.25(15)
C(11)−Ru−C(14)	77.46(16)	C(2)−Ru−C(13)	95.20(18)
C(6)−Ru−C(13)	109.55(19)	C(10)−Ru−C(13)	78.21(14)
C(12)−Ru−C(13)	36.48(15)	C(15)−Ru−C(13)	65.53(15)
C(14)−Ru−C(13)	36.49(14)	C(10)−Ru−C(1)	155.86(17)
C(2)−Ru−C(1)	36.40(17)	C(6)−Ru−C(1)	67.5(2)
C(12)−Ru−C(1)	129.22(17)	C(15)−Ru−C(1)	122.10(18)
C(11)−Ru−C(1)	165.12(17)	C(13)−Ru−C(1)	104.52(18)
C(14)−Ru−C(1)	101.64(18)	C(2)−Ru−P(1)	107.94(15)
C(6)−Ru−P(1)	93.15(15)	C(10)−Ru−P(1)	80.21(10)
C(12)−Ru−P(1)	138.20(11)	C(15)−Ru−P(1)	90.79(11)
C(11)−Ru−P(1)	101.91(10)	C(14)−Ru−P(1)	123.11(11)
C(13)−Ru−P(1)	156.00(11)	C(1)−Ru−P(1)	91.06(14)
C(8)−P(1)−C(22)	103.10(16)	C(8)−P(1)−Ru	104.00(12)
C(22)−P(1)−Ru	121.35(10)	C(6)−C(2)−C(1)	126.6(5)

approximately 50:50 about a pseudo-mirror and failed to refine well due to high correlation. The observation of an ordered structure for the allyl ligand in **6** is due to the fact that the steric environment induced by the two phenyl groups attached to the phosphine atom is not symmetrical. Consequently, one face of the allyl is preferentially coordinated to the metal.

Table 3. Selected Bond Lengths (Å) and Angles (deg) for 6

Bond Lengths			
Ru−C(2)	2.188(4)	Ru−C(10)	2.211(5)
Ru−C(6)	2.228(5)	Ru−C(11)	2.232(5)
Ru−C(1)	2.243(4)	Ru−C(12)	2.240(5)
Ru−C(14)	2.243(5)	Ru−C(15)	2.256(5)
Ru−C(13)	2.267(5)	Ru−P(1)	2.3062(12)
C(1)−C(2)	1.404(6)	C(2)−C(6)	1.396(6)

Bond Angles			
C(2)−Ru−C(10)	174.95(18)	C(2)−Ru−C(6)	36.85(16)
C(10)−Ru−C(6)	145.87(19)	C(2)−Ru−C(11)	142.1(2)
C(10)−Ru−C(11)	36.97(19)	C(6)−Ru−C(11)	113.2(2)
C(2)−Ru−C(1)	36.91(16)	C(10)−Ru−C(1)	143.86(18)
C(6)−Ru−C(1)	66.58(17)	C(11)−Ru−C(1)	178.28(18)
C(2)−Ru−C(12)	110.13(19)	C(10)−Ru−C(12)	66.7(2)
C(6)−Ru−C(12)	97.25(19)	C(11)−Ru−C12)	37.23(19)
C(1)−Ru−C(12)	141.08(18)	C(2)−Ru−C(14)	109.7(2)
C(10)−Ru−C(14)	65.5(2)	C(6)−Ru−C(14)	137.0(2)
C(11)−Ru−C(14)	77.5(2)	C(1)−Ru−C(14)	101.52(19)
C(12)−Ru−C(14)	65.5(2)	C(2)−Ru−C(15)	140.03(19)
C(10)−Ru−C(15)	36.45(19)	C(6)−Ru−C(15)	172.61(19)
C(11)−Ru−C(15)	65.7(2)	C(1)−Ru−C(15)	114.30(18)
C(12)−Ru−C(15)	77.5(2)	C(14)−Ru−C(15)	35.9(2)
C(2)−Ru−C(13)	97.30(18)	C(10)−Ru−C(13)	77.83(19)
C(6)−Ru−C(13)	107.92(19)	C(11)−Ru−C(13)	66.24(19)
C(1)−Ru−C(13)	112.13(18)	C(12)−Ru−C(13)	36.78(19)
C(14)−Ru−C(13)	35.79(19)	C(15)−Ru−C(13)	64.8(2)
C(2)−Ru−P(1)	105.55(12)	C(10)−Ru−P(1)	79.31(14)
C(6)−Ru−P(1)	91.32(12)	C(11)−Ru−P(1)	95.20(14)
C(1)−Ru−P(1)	86.52(11)	C(12)−Ru−P(1)	130.64(15)
C(14)−Ru−P(1)	130.36(16)	C(15)−Ru−P(1)	96.05(15)
C(13)−Ru−P(1)	157.13(14)	C(8)−P(1)−Ru	104.65(16)
C(2)−C(1)−Ru	69.4(2)	C(5)−C(1)−Ru	119.4(3)
C(6)−C(2)−C(1)	122.4(4)	C(6)−C(2)−Ru	73.1(3)
C(1)−C(2)−Ru	73.7(2)		

The C1−C2 and C2−C6 bond distances for **5** are 1.414(6) and 1.404(6) Å, respectively, and those for **6** are 1.404(6) and 1.396(6) Å, respectively. These bond distances are typical for conjugated double bonds.[46] The bond angles C(1)−C(2)−C(6) are 126.6(5) (**5**) and 122.4(4)° (**6**), which are close to the ideal sp^2 bond angle of 120°. The bond distances Ru−C(1), Ru−C(2), and Ru−C(6) of **5** and **6** are similar: 2.313(6), 2.203(7), and 2.218(6) Å, respectively, for **5** and 2.243(4), 2.188(4), and 2.228(5) Å, respectively, for **6**. The bond distances from ruthenium to the coordinated arene for **5** are as follows: 2.219(3) Å, Ru−C(10). 2.241(3) Å, Ru−C(11); 2.230(3) Å, Ru−C(12); 2.257(4) Å, Ru−C(13); 2.246(4) Å, Ru−C(14); 2.238(3) Å, Ru−C(15). Similarly, the distance for **6** are as follows: 2.211(5) Å, Ru−C(10); 2.232(5) Å, Ru−C(11); 2.240(5) Å, Ru−C(12); 2.267(5) Å, Ru−C(13); 2.243(5) Å, Ru−C(14); 2.256(5) Å, Ru−C(15). As observed for **1**[36] and **3**, the constraint of the two-carbon bridge probably gives rise to the elongated Ru−C(13) distance trans to the bridge and the shortened Ru−C(10) distance adjacent to the bridge. Further comparison of the structures of **5** and **6** reveals that the relative positions of the allyl ligands and the coordinated arenes are different: complex **5** shows a slightly staggered conformation, and complex **6** shows an eclipsed conformation. The difference probably arises from the differing steric effects of the phosphine ligands. The

(46) Streitwieser, A., Jr.; Heathcock, C. H. *Introduction to Organic Chemistry*; Macmillan: New York, 1981.

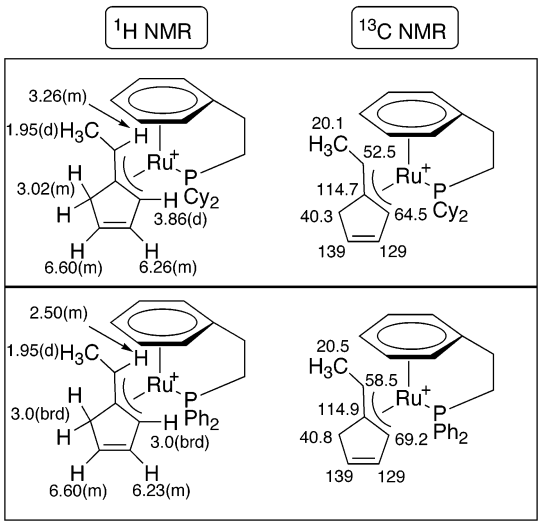

Figure 4. Chemical shift assignments for the allyl ligands of **5** (top) and **6** (bottom) in CD_2Cl_2.

space-filling structure of **6** suggests steric hindrance between the allylic carbons (C1 and C6) and the phenyl ring attached to phosphorus, which probably prevents the type of staggered conformation observed for **5**.

Compounds **5** and **6** were also characterized by ^{1}H, ^{13}C, ^{1}H−^{1}H COSY, and ^{1}H−^{13}C COSY NMR spectroscopy. Figure 4 shows the chemical shift assignments for the η^3-allyl ligands of **5** and **6** determined from these studies. The assignments are consistent with those of analogous metal allyls reported in the literature.[4,47,48] The coordinated arenes exhibit five distinct ^{1}H NMR resonances for each compound: δ 5.93 (d), 5.79 (d), 5.50 (t), 5.12 (t), and 3.94 (t) for compound **5**, and δ 6.12 (d), 5.91 (d), 5.81 (t), 5.28 (t), and 4.20 (t) for compound **6**.

Mechanism of the Oligomerization/Polymerization of HC≡CH. The metal-mediated oligomerization/polymerization of alkynes has been shown to occur via at least three distinct pathways. The first involves alkyne insertion into the M−CY=CYX bond (Y = H, R; X = H, R, Cl).[49,50,62,63] The second involves alkyne metathesis of metal−carbene complexes.[51−53] The third involves coordination of two molecules of alkyne followed by the formation of a metallocyclopentadiene.[11,12] While only a few examples of alkyne insertion into Ru−alkyl bonds have been reported,[54,55] alkyne insertion into Ru−hydride bonds is well-known.[56−59] The relative paucity of examples of the former reaction is probably due to the high energy barrier to insertion into Ru−alkyl bonds relative to that for Ru−H bonds.[60] For these reasons, we chose to examine the mechanism of acetylene oligomerization/polymerization observed in the present system.

To probe the mechanism of this reaction, we synthesized the deuterium-labeled dialkyl compound (η^6:η^1-$C_6H_5CH_2CH_2PPh_2$)$Ru(CD_3)_2$ (**2**-d_6), which was prepared using a procedure analogous to that used to prepare (η^6:η^1-$C_6H_5CH_2CH_2PPh_2$)$Ru(CH_3)_2$ (**2**).[36] Upon the reaction of **2**-d_6 with $\mathbf{H^+B^-}$ in the presence of acetylene, the complex [(η^6:η^1-$C_6H_5CH_2CH_2PPh_2$)Ru(η^3-$CD_3CHC_5H_5$)]-[B(3,5-$C_6H_3(CF_3)_2)_4$] was obtained (see eq 3). Since the

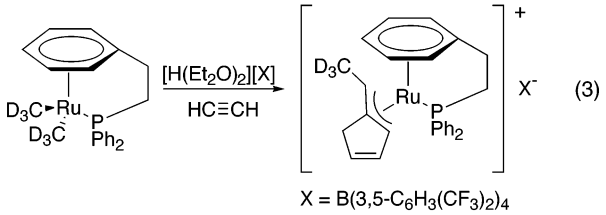

(3)

reaction of **2** with $\mathbf{H^+B^-}$ in the presence of CO produced predominantly (η^6:η^1-$C_6H_5CH_2CH_2PPh_2$)$RuCH_3(CO)$ (**4**) as judged by ^{1}H NMR spectroscopy, we can infer that $\mathbf{H^+B^-}$ fails to generate, at least in any substantial amounts,[61] methylidene intermediates via hydride abstraction from methyl as proposed for the reaction of the related dimethyl complexes with Ph_3CX (X = PF_6^-, BF_4^-).[37−40]

These considerations and other literature precedents[62−65] have led us to propose the mechanism in Scheme 1 to rationalize the formation of complexes **5** and **6**. Abstraction of one of the methide ligands of **1** or **2** by $\mathbf{H^+B^-}$ followed by coordination of acetylene gives intermediate **i**. Insertion of acetylene into the Ru−CH_3 bond[63] followed again by coordination of acetylene gives intermediate **ii**, in which the stereochemistry of the alkene is either cis or trans. The polyacetylenes are probably obtained by repeated acetylene insertions

(47) Nagashima, H.; Mukai, K.; Shiota, Y.; Yamaguchi, K.; Ara, K.; Fukahori, T.; Suzuki, H.; Akita, M.; Moro-ka, Y.; Itoh, K. *Organometallics* **1990**, *9*, 799.
(48) Albers, M. O.; Liles, D. C.; Robinson, D. J.; Shaver, A.; Singleton, E. *Organometallics* **1987**, *6*, 2347.
(49) Keim, W.; Behr, A.; Pöper, M. In *Comprehensive Organometallic Chemistry I*; Wilkinson, G.; Stone, F. G. A.; Abel, E. W., Eds.; Pergamon: 1982; Vol. 8, p 371.
(50) Clarke, T. C.; Yannoni, C. S.; Katz, T. J. *J. Am. Chem. Soc.* **1983**, *105*, 7787.
(51) Strutz, H.; Dewan, J. C.; Schrock, R. R. J. *J. Am. Chem. Soc.* **1985**, *107*, 5999.
(52) Schlund, R.; Schrock, R. R.; Crowe, W. E. *J. Am. Chem. Soc.* **1989**, *111*, 8004.
(53) Park, L. Y.; Schrock, R. R.; Stieglits, S. G.; Crowe, W. E. *Macromolecules* **1991**, *24*, 3180.
(54) Crook, J. R. *J. Chem. Soc., Dalton Trans.* **1989**, 465.
(55) Bruce, M. I.; Gardner, R. C. F.; Stone, G. A. *J. Chem. Soc., Dalton Trans.* **1979**, 906.
(56) Torres, M. R.; Vegas, A.; Santos, A. *J. Organomet. Chem.* **1986**, *309*, 169.
(57) Castano, A. M.; Echavarren, A. M. *J. Organomet. Chem.* **1989**, *379*, 171.
(58) Harris, M. C. J.; Hill, A. F. *Organometallics* **1991**, *10*, 3903.
(59) Blackmore, T.; Bruce, M. I.; Stone, F. G. A. *J. Chem. Soc., Dalton Trans.* **1974**, 106.
(60) Siegbahn, E. M. *Chem. Phys. Lett.* **1993**, *205*, 290.
(61) From later studies of the reaction of **2** with $\mathbf{H^+B^-}$ in the presence of norbornene (vide infra), we infer that methylidene intermediates are, in fact, generated because we observe the production of ring-opened polynorbornene. These intermediates are, however, apparently generated in only trace amounts, given the fact that we observe the clean production of **4** from **2** in the presence of CO (vide supra) and the fact that we can detect by ^{1}H NMR spectroscopy no species attributable to Ru−methylidenes in any of the reactions examined in this report.
(62) Dietl, H.; Reinheimer, H.; Moffat, J.; Maitlis, P. M. *J. Am. Chem. Soc.* **1970**, *92*, 2276.
(63) Henry, P. M. *Adv. Organomet. Chem.* **1975**, *13*, 363.
(64) The coordination of $CH_3CH{=}C_5H_4$ probably occurs via one of the double bonds in the five-membered ring because the endocyclic double bonds are electron-rich due to the aromaticity of the resonance structure

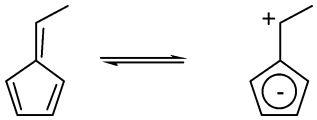

(65) Gavens, P. D.; Botlrill, M.; Kelland, J. W.; McMeeking, J. In *Comprehensive Organometallic Chemistry I*; Wilkinson, G., Stone, F. G. A., Abel, E. W., Eds.; Pergamon: New York, 1982; Vol. 3, p 475.

Scheme 1

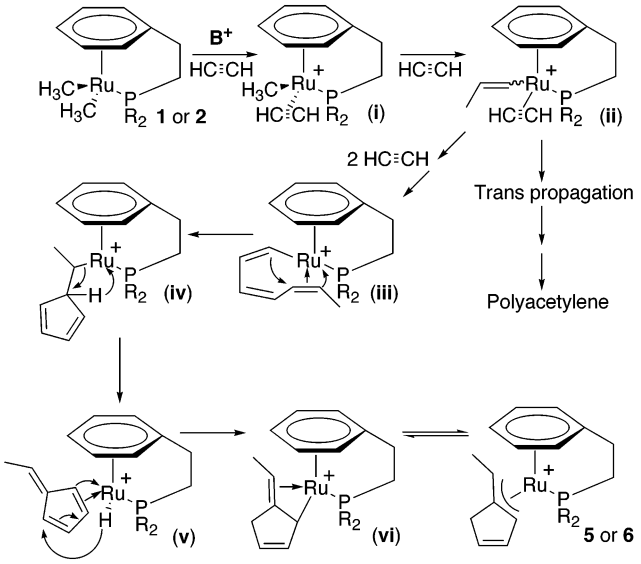

Scheme 2

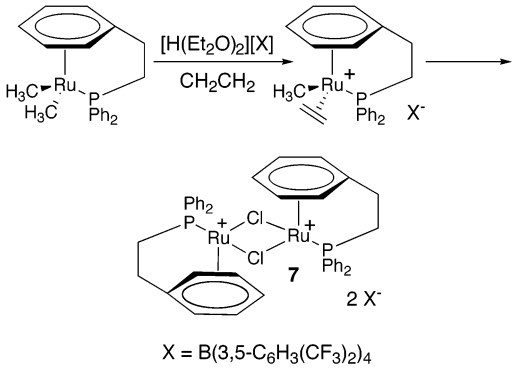

through trans configurations until an undefined termination reaction occurs. We propose trans propagation for this process because it would place the distal alkene away from the metal, which would discourage Ru-mediated termination reactions during the initial steps. Starting with intermediate **ii**, in which the alkene possesses a trans configuration, two successive cis insertions of acetylene affords intermediate **iii**. These steps orient the distal alkene in a position that permits coordination to the metal center. Intermediate **iii** then undergoes insertion of the coordinating distal alkene into the Ru−alkyl bond to form a five-membered ring. A related pathway was proposed in the catalytic reaction of acetylene with $(PhCN)_2PdCl_2$ to produce six-membered rings.[62,63] Intermediate **iv** then undergoes β-hydride elimination to produce a free five-membered ring that recoordinates to the ruthenium center, forming intermediate **v**.[64] Insertion of the resulting diene into the Ru−H bond gives the $\sigma-\pi$ allyl intermediate **vi**,[49,65] which converts to the more thermodynamically stable isomer (i.e., **5** or **6**).

Reaction of 1 and 2 with H^+B^- in the Presence of Ethylene. The reaction of complex **1** with H^+B^- in CD_2Cl_2 under 1 atm of ethylene initially afforded an unidentified monomethyl Ru complex. For this complex, we assign the doublet appearing at δ 0.05 (d, $J_{HP} = 5.7$ Hz, 3 H) to the Ru*CH*$_3$ group and the four distinct resonances appearing at δ 6.17 (t, $J_{HH} = 5.4$ Hz, 1 H), 6.06 (m, 2 H), 5.67 (d, $J_{HH} = 5.4$ Hz, 1 H), and 5.34 (t, $J_{HH} = 5.4$ Hz, 1 H) to the coordinated arene. These resonances were observed to gradually diminish and/or shift over time. After 23 h, the cationic olefin−hydride complex $[(\eta^6{:}\eta^1\text{-}C_6H_5CH_2CH_2PCy_2)RuH(CH_2{=}CH_2)]^+$ was observed in solution. This complex was previously obtained from the reaction of **1** with CPh_3PF_6, apparently through the intermediacy of Ru−methylidene and Ru−ethyl species.[36] While the complexity of the ^{1}H NMR spectra (due to apparent side reactions occurring during the transformation) precluded a detailed analysis of the pathway by which the olefin complex formed in the present study, we can speculate, on the basis of the studies described above, that the reaction proceeds via a four-step process involving (1) abstraction of a methide ligand from **1**, (2) coordination and insertion of ethylene into the remaining Ru−CH_3 bond, (3) β-hydride elimination, and (4) replacement of the thus generated propylene ligand with ethylene, which is present in excess.

The reaction of complex **2** with H^+B^- in CD_2Cl_2 under 1 atm of ethylene initially afforded the cationic olefin−methyl complex $[(\eta^6{:}\eta^1\text{-}C_6H_5CH_2CH_2PPh_2)RuCH_3(CH_2{=}CH_2)][B(3,5\text{-}C_6H_3(CF_3)_2)_4]$. We assign the resonance at δ −0.53 (d, $J_{HP} = 7.8$ Hz, 3 H) to the Ru*CH*$_3$ group and the multiplets at δ 2.03 and 3.40 to the coordinated ethylene group. We further assign the resonances at δ 6.35 (m, 2 H), 6.28 (t, 1 H), 5.78 (d, 1 H), and 5.61 ppm (t, 1 H) to the coordinated arene group and the two multiplets at δ 3.18 and 2.69 to the hydrogens of the two-carbon bridge. We were unable to isolate this cationic olefin−methyl complex due to its facile decomposition at room temperature in both CH_2Cl_2 and CD_2Cl_2. The color of the solution gradually changed from light yellow to reddish brown; meanwhile, the Ru*CH*$_3$ resonance gradually diminished in intensity, and new resonances appeared at δ 5.16 (br, 1 H), 5.87 (br, 1 H), 6.46 (br, 1 H), and 6.58 (br, 2 H) and at δ −7.6 (d, $J_{HP} = 28$ Hz, 1 H). We infer that these resonances correspond to coordinated arene and Ru*H* moieties, respectively.

The broadening of the resonances in the ^{1}H NMR spectra during the decomposition prevented any further detailed analysis of the reaction. We therefore sought to isolate and analyze the products of the decomposition. Consequently, a freshly prepared sample of $[(\eta^6{:}\eta^1\text{-}C_6H_5CH_2CH_2PPh_2)RuCH_3(CH_2{=}CH_2)][B(3,5\text{-}C_6H_3(CF_3)_2)_4]$ was dissolved in CH_2Cl_2. After the complete disappearance of the Ru*CH*$_3$ resonance (approximately 2 days), the reaction mixture was concentrated, and an aliquot of hexanes was added to induce crystallization. Analysis of the resulting red crystals by X-ray crystallography revealed the structure of the predominant (i.e., ≥50%) decomposition product to be the dimer $[(\eta^6{:}\eta^1\text{-}C_6H_5CH_2CH_2PPh_2)RuCl]_2[B(3,5\text{-}C_6H_3(CF_3)_2)_4]_2$ (**7**) (Scheme 2).

The thermal ellipsoid plot obtained for **7** is shown in Figure 5; selected bond distances and angles are provided in Table 4. The molecule possesses a center of inversion between the two chlorine atoms. The Ru−Cl bond distance, 2.4341(8) Å, is similar to those reported in the literature for analogous bridging-chloride systems.[43,66] The coordinated arene is slightly tilted due to the constraint of the two-carbon bridge, as was

(66) Gusev, O.; Ievlev, M. A.; Lyssenko, K. A.; Petrovskii, P. V.; Ustynyuk, N. A.; Maitlis, P. M. *Inorg. Chim. Acta* **1998**, *280*, 249.

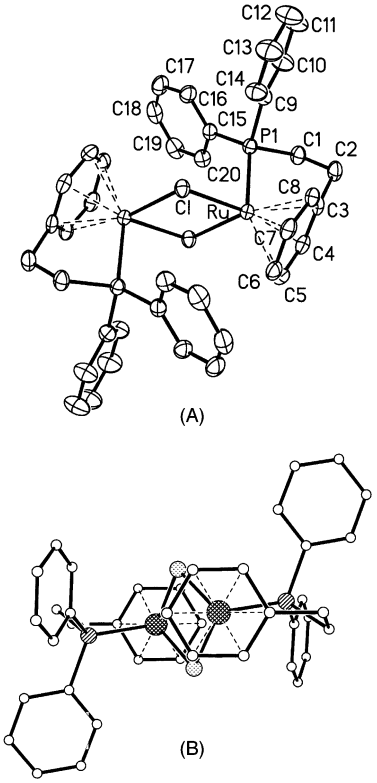

Figure 5. Thermal ellipsoid plot of $[(\eta^6{:}\eta^1\text{-}C_6H_5CH_2CH_2PPh_2)RuCl]_2[B(3,5\text{-}C_6H_3(CF_3)_2)_4]_2$ (**7**) at the 40% probability level.

Table 4. Selected Bond Lengths (Å) and Angles (deg) for 7

	Bond Lengths		
Ru−C(3)	2.182(3)	Ru−C(4)	2.194(3)
Ru−C(7)	2.202(4)	Ru−C(8)	2.205(3)
Ru−C(5)	2.243(4)	Ru−C(6)	2.276(4)
Ru−P(1)	2.3624(9)	Ru−Cl	2.4363(8)
Ru−Cl#1	2.4341(8)	Cl−Ru#1	2.4341(8)
	Bond Angles		
C(3)−Ru−C(4)	37.63(13)	C(3)−Ru−C(7)	68.07(13)
C(4)−Ru−C(7)	79.49(13)	C(3)−Ru−C(8)	38.05(12)
C(4)−Ru−C(8)	67.64(13)	C(7)−Ru−C(8)	37.29(13)
C(3)−Ru−C(5)	67.57(13)	C(4)−Ru−C(5)	37.48(13)
C(7)−Ru−C(5)	66.02(15)	C(8)−Ru−C(5)	78.82(14)
C(3)−Ru−C(6)	79.61(13)	C(4)−Ru−C(6)	66.54(13)
C(7)−Ru−C(6)	36.97(14)	C(8)−Ru−C(6)	66.77(14)
C(5)−Ru−C(6)	35.90(14)	C(3)−Ru−P(1)	79.04(10)
C(4)−Ru−P(1)	100.12(10)	C(7)−Ru−P(1)	125.34(10)
C(8)−Ru−P(1)	91.43(10)	C(5)−Ru−P(1)	137.05(10)
C(6)−Ru−P(1)	157.28(9)	C(3)−Ru−Cl#1	132.60(9)
C(4)−Ru−Cl#1	100.43(10)	C(7)−Ru−Cl#1	140.45(10)
C(8)−Ru−Cl#1	167.67(9)	C(5)−Ru−Cl#1	89.75(10)
C(6)−Ru−Cl#1	106.32(10)	P(1)−Ru−Cl#1	93.87(3)
C(3)−Ru−Cl	146.42(10)	C(4)−Ru−Cl	166.78(10)
C(7)−Ru−Cl	91.70(9)	C(8)−Ru−Cl	110.80(9)
C(5)−Ru−Cl	129.66(10)	C(6)−Ru−Cl	100.53(9)
P(1)−Ru−Cl	93.01(3)	Cl#1−Ru−Cl	80.05(3)
Ru#1−Cl−Ru	99.95(3)		

observed for complexes **1**,[36] **3**, **5**, and **6** (vide supra). Consequently, the Ru−C(3) bond distance is shorter than those of the remaining five Ru−C arene bond distances.

The formation of $[(\eta^6\text{-}C_6Me_6)RuCH_3(CH_2{=}CH_2)PR_3]$, where R = Me, Ph, was previously observed by Werner and co-workers from the reaction of $(\eta^6\text{-}C_6Me_6)Ru(CH_3)_2PR_3$ with HBF_4 in the presence of ethylene.[39] Similar to our findings, these researchers were unable to isolate the analogous intermediate $[(\eta^6\text{-}C_6Me_6)RuCH_3(CH_2{=}CH_2)PPh_3][BF_4]$ due to its facile decomposition. However, the decomposition product $[(\eta^6\text{-}C_6Me_6)RuH(PPh_2\text{-}C_6H_4CH{=}CH_2)][BF_4]$ was isolated and was proposed to form through a three-step process involving (1) ortho metalation, (2) insertion of ethylene into the ortho-metalated bond, and (3) β-hydride elimination.[36] Although ortho metalation is a common pathway for the decomposition of coordinatively unsaturated metal alkyls that contain aromatic ligands,[67−73] we observed no ortho metalation reactions involving complex **2** or any of its derivatives. It is apparent that the tethered arene−phosphine ligand inhibits ortho metalation, which suggests a greater stability of the tethered cationic species relative to analogous nontethered cationic species.[36] The rigid structure of the tethered arene−phosphine ligand probably prevents interaction between the metal and the ortho C−H bond.

At present, we are unable to provide experimental support for any proposed reaction pathway that might lead to the formation of complex **7**. We can speculate, however, that the reaction(s) leading directly to **7** is (are) probably preceded by the reaction of CH_2Cl_2 with $[(\eta^6{:}\eta^1\text{-}C_6H_5CH_2CH_2PPh_2)RuH(CH_3CH{=}CH_2)][B(3,5\text{-}C_6H_3(CF_3)_2)_4]$.[74] It is known that transition-metal hydrides react with haloalkanes to give the corresponding transition-metal halides with concurrent reduction of the haloalkanes.[75−79] Furthermore, the observed reactions of $HMn(CO)_4PPh_3$[76] with various haloalkanes and the reaction of $HOs(CO)_4Os(CO)_4R$[77] with CCl_4 have been rationalized on the basis of pathways involving radical species.

Reaction of 1 and 2 with Various Methide-Abstraction Agents in the Presence of Norbornene. In CH_2Cl_2, the reaction of complexes **1** and **2** with $\mathbf{H^+B^-}$, $B(C_6F_5)_3$, and Ph_3CBF_4 in the presence of norbornene at ambient temperature produced ring-opened polynorbornene (eq 4). Analysis by ^1H NMR spectroscopy

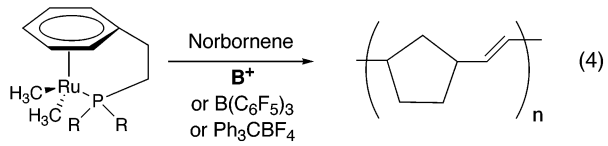

(4)

($CDCl_3$) of the olefinic region showed two resonances at δ 5.19 and 5.34 corresponding to the cis and trans olefins, respectively.[79] Integration of the spectra revealed that 90% of the double bonds were trans, as has

(67) Bruce, M. I. *Angew. Chem., Int. Ed. Engl.* **1977**, *16*, 73.
(68) Constable, E. C. *Polyhedron* **1984**, *3*, 1037.
(69) Horiie, S.; Murahashi, S. *Bull. Chem. Soc. Jpn.* **1960**, *23*, 247.
(70) Kleiman, J. P.; Dubeck, M. *J. Am. Chem. Soc.* **1963**, *85*, 1544.
(71) Bennett, M. A.; Milner, D. L. *J. Am. Chem. Soc.* **1969**, *91*, 6983.
(72) Advasio, V.; Diversi, P.; Ingrosso, G.; Lucherini, A.; Marchetti, F.; Nardelli, M. *J. Chem. Soc., Dalton Trans.* **1992**, 3385.
(73) Diversi, P.; Ingrosso, G.; Lucherini, A.; Marchetti, F.; Adovasio, V.; Nardelli, M. *J. Chem. Soc., Dalton Trans.* **1990**, 1779.
(74) Although we were unable to identify any ^1H NMR resonances specifically assignable to the complex $[(\eta^6{:}\eta^1\text{-}C_6H_5CH_2CH_2PPh_2)RuH(CH_3\text{-}CH{=}CH_2)][B(3,5\text{-}C_6H_3(CF_3)_2)_4]$ because of peak broadening over the ranges δ 2.3−2.7 and 3.1−3.6, this species can plausibly form via the insertion of ethylene into a $Ru-CH_3$ bond followed by β-hydride elimination.
(75) Green, M. L. H.; Wong, L. *J. Chem. Soc., Chem. Commun.* **1984**, 1442.
(76) Booth, B. L.; Shaw, B. L. *J. Organomet. Chem.* **1972**, *43*, 369.
(77) Carter, W. J.; Kelland, J. W.; Okrasinski, S. J.; Warner, K. E.; Norton, J. R. *Inorg. Chem.* **1982**, *21*, 3955.
(78) Booth, B. L.; Haszeldine, R. N. *J. Chem. Soc.* **1966**, 157.
(79) Wache, S. *J. Organomet. Chem.* **1995**, *494*, 235.

Table 5. Polymerization of Norbornene in the Presence of Activated 1 and 2

entry	complex	activator	yield (%)	$10^{-3}M_n$	$10^{-3}M_w$	PDI
1	**1**	$\mathbf{H^+B^-}$	51	42	117	2.77
2	**1**	$B(C_6F_5)_3$	21	74	163	2.21
3	**1**	Ph_3CBF_4	85	106	198	1.87
4	**2**	$\mathbf{H^+B^-}$	10	196	469	2.39
5	**2**	$B(C_6F_5)_3$	8.5	101	233	2.30
6	**2**	Ph_3CBF_4	17	208	321	1.54

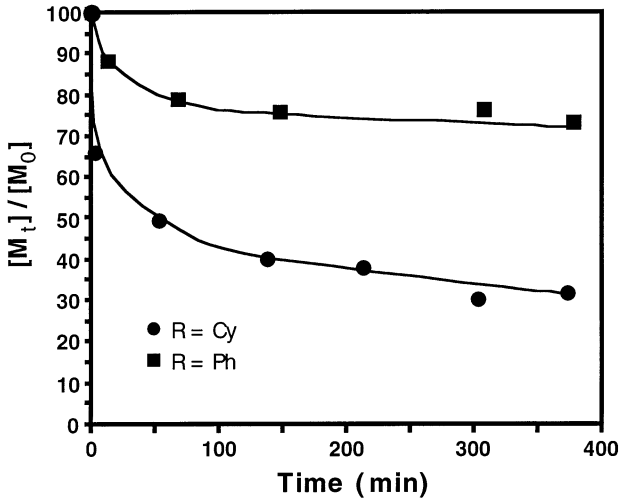

Figure 6. Time dependence of monomer consumption during the polymerization of norbornene using $(\eta^6{:}\eta^1\text{-}C_6H_5CH_2CH_2PR_2)Ru(CH_3)_2$ (R = Cy, Ph) activated with Ph_3CBF_4. M_t = monomer at time t. M_0 = monomer at time zero.

been observed in the polymerization of norbornene using other Ru-based ROMP initiators.[80−82] The M_w, M_n, and polydispersity index (PDI) values of the polymers were measured by gel permeation chromatography (GPC) and are listed in Table 5. With all three activators, complex **1** exhibited greater polymerization activity than complex **2**. Furthermore, the highest molecular weights and lowest PDIs were obtained using the activator Ph_3CBF_4, demonstrating the enhanced efficiency of this activator relative to that of the other boron activators.

Figure 6 shows the time dependence of the consumption of monomer, which was monitored by ^{1}H NMR spectroscopy in CD_2Cl_2. Complex **1**, when activated with Ph_3CBF_4, showed substantial consumption of monomer (∼34%) during the first 5 min of polymerization. The rate of polymerization was then substantially slower, with ∼36% of the monomer consumed during the next 6 h. The same trend was observed with the other boron activators, although the activity was markedly lower. We were unable to conduct a detailed kinetic study with these systems because gelation occurred during the course of the polymerizations. Gelation undoubtedly slows the rate of polymerization by inhibiting monomer diffusion to the active site.[83]

While metal alkylidenes are known to be the active species in metal-catalyzed olefin metathesis reactions,[82] we were unable to detect any ^{1}H NMR resonances attributable to ruthenium alkylidenes in the polymerizations reported here. Previously, however, we showed that the reaction of complexes **1** and **2** with Ph_3CPF_6 produced the cationic olefin complexes $[(\eta^6{:}\eta^1\text{-}C_6H_5CH_2CH_2PR_2)RuH(CH_2{=}CH_2)]^+$ (R = Cy, Ph, respectively).[36] In these studies, we proposed that the products formed via the intermediacy of ruthenium methylidene species. Likewise, we propose that Ru−methylidene intermediates serve as the active ROMP initiators in the present polymerization reactions. The greater activity of Ph_3CPF_6 compared to the boron activators probably arises because the latter activators preferentially abstract a methide from **1** and **2** (vide supra), while Ph_3CPF_6 preferentially abstracts a hydride from **1** and **2**.[4,36,39,40]

Conclusions

We obtained the complexes $(\eta^6{:}\eta^1\text{-}C_6H_5CH_2CH_2PR_2)Ru(CH_3)(CO)$ and $[(\eta^6{:}\eta^1\text{-}C_6H_5CH_2CH_2PR_2)Ru(\eta^3\text{-}CH_3CHC_5H_5)][B(3,5\text{-}C_6H_3(CF_3)_2)_4]$ by the reaction of $(\eta^6{:}\eta^1\text{-}C_6H_5CH_2CH_2PR_2)Ru(CH_3)_2$, where R = Cy (**1**), Ph (**2**), with $H(Et_2O)_2[B(3,5\text{-}C_6H_3(CF_3)_2)_4]$ ($\mathbf{H^+B^-}$) in the presence of CO and acetylene, respectively. In the reactions with acetylene, polyacetylene was also obtained as a major product. Initial insertion of acetylene into a Ru−CH_3 bond followed by trimerization and/or polymerization of acetylene apparently gave rise to the observed products. In contrast, similar reaction of **2** with $\mathbf{H^+B^-}$ in the presence of ethylene initially produced $[(\eta^6{:}\eta^1\text{-}C_6H_5CH_2CH_2PPh_2)RuCH_3(CH_2{=}CH_2)][B(3,5\text{-}C_6H_3(CF_3)_2)_4]$, which decomposed to give the dimer $[(\eta^6{:}\eta^1\text{-}C_6H_5CH_2CH_2PPh_2)RuCl]_2[B(3,5\text{-}C_6H_3(CF_3)_2)_4]_2$. Similar reaction of **1** and **2** with $\mathbf{H^+B^-}$ in the presence of norbornene afforded ring-opened polynorbornene. Collectively, these results demonstrate that two distinct classes of olefin polymerization can be catalyzed by selective in situ derivatization of complexes **1** and **2**.

Experimental Section

Materials and Methods. Before use, all solvents were dried by passage through alumina and degassed by freeze−pump−thaw methods. The chemicals methyllithium-d_3, norbornene, and triphenylcarbenium tetrafluoroborate (Ph_3CBF_4) were purchased from Aldrich Chemical Co. Similarly, tris(pentafluorophenyl)borate ($B(C_6F_5)_3$) was purchased from Strem Chemical Co., and acetylene (99.8% purity), carbon monoxide (99.9% purity), and ethylene (polymerization grade) were purchased from Matheson-Trigas. The compounds diethyloxonium tetrakis[tris(fluoromethyl)phenyl]borate ($[H(Et_2O)_2][B(3,5\text{-}C_6H_3(CF_3)_2)_4]$, $\mathbf{H^+B^-}$)[84] and $(\eta^6{:}\eta^1\text{-}C_6H_5CH_2CH_2PR_2)Ru(CH_3)_2$, where R = Cy (**1**), Ph (**2**),[36] were prepared according to the indicated literature procedures. While we report a satisfactory elemental analysis for the new complex **3**, we did not attempt to perform elemental analyses on complexes **4**−**6** because crystalline samples of these complexes could not be readily separated from the oily residues in which the crystals grew (vide supra). Furthermore, we were unable to obtain a satisfactory analysis for complex **7**, apparently due to contamination by an uncharacterized Ru−H side product (vide infra). Nuclear magnetic resonance (NMR) spectra were recorded on a General Electric QE-300 spectrometer operating at 300 MHz (for ^{1}H) and 75.5 MHz (for ^{13}C). Chemical shifts are reported in units of δ (ppm) relative to residual isotopic

(80) Ivin, K. J.; Laverty, D. T.; Rooney, J. *J. Makromol. Chem.* **1977**, *178*, 1545.
(81) Schwab, P.; Grubbs, R. H.; Ziller, J. W. *J. Am. Chem. Soc.* **1996**, *118*, 100.
(82) Moore, J. S. In *Comprehensive Organometallic Chemistry II*; Abel, E. W., Stone, F. G. A., Wilkinson, G., Eds.; Hegedus, L., Vol. Ed.; Pergamon: New York, 1995; Vol. 12, p 1209.
(83) Odian, G. *Principles of Polymerization*; Wiley: New York, 1981.
(84) Brookhart, M.; Grant, B.; Volpe, A. F., Jr. *Organometallics* **1992**, *11*, 3920.

impurities in the solvents. Infrared (IR) spectra were recorded on a Mattson Galaxy Serio FTIR 5000. Elemental analyses were performed by Oneida Research.

Synthesis of [(η^6:η^1-$C_6H_5CH_2CH_2PCy_2$)RuCH$_3$CO][B(3,5-$C_6H_3(CF_3)_2)_4$] (3). A solution of 0.10 g (2.3×10^{-4} mol) of **1** in CH_2Cl_2 (20 mL) was bubbled with CO at −76 °C for 3 min. To this solution was added an aliquot of $\mathbf{H^+B^-}$ (0.21 g; 2.1×10^{-4} mol) in CH_2Cl_2 (5 mL) at −76 °C, and the solution was slowly warmed to room temperature and stirred for 15 min. The solution was concentrated to ∼5 mL under vacuum, and hexanes were added to precipitate fine light yellow crystals. The crystals were collected by filtration and dried under vacuum. Yield: 0.067 g; 23%. ^{1}H NMR (CD_2Cl_2; 300 MHz; 293 K): δ 7.72 (s, 8 H, B(3,5-C_6H_3(CF_3)$_2$)$_4$), 7.56 (s, 4 H, B(3,5-C_6H_3-(CF_3)$_2$)$_4$), 6.39 (m, 2 H, η^6-C_6H_5), 6.14 (d, J_{HH} = 6.3 Hz, 1 H, η^6-C_6H_5), 6.03 (m, 2 H, η^6-C_6H_5), 2.96 (m, 1 H, $C_6H_5CH_2CH_2P$), 2.83 (m, 1 H, $C_6H_5CH_2CH_2P$), 2.59 (m, 2 H, $C_6H_5CH_2CH_2P$), 1.27−2.10 (m, 22 H, *Cy*$_2$), 0.53 (d, J_{PH} = 3.0 Hz, 3 H, Ru−*CH*$_3$). ^{13}C NMR (CD_2Cl_2; 75.5 MHz; 293 K): δ 198.01, 162.35 (q, J_{CB} = 79.7 Hz), 135.39, 134.76, 129.23 (q, $^2J_{CF}$ = 25.1 Hz), 124.49 (q, $^1J_{CF}$ = 272.7 Hz), 118.07, 110.96, 98.52, 97.87, 92.62, 92.41, 41.28 (d, J_{CP} = 29.4 Hz), 36.42 (d, J_{CP} = 27.3 Hz), 33.59 (d, J_{CP} = 23 Hz), 31.50, 26.1−28.9 (m), −22.01. IR (Nujol, cm^{-1}): 2017, 1278, 1126, 887, 839. Anal. Calcd for $C_{54}H_{46}$-$RuPOBF_{24}$: C, 49.47; H, 3.51. Found: C, 49.21; H, 3.22.

Synthesis of [(η^6:η^1-$C_6H_5CH_2CH_2PPh_2$)RuCH$_3$CO][B(3,5-$C_6H_3(CF_3)_2)_4$] (4). A solution of 0.10 g (2.4×10^{-4} mol) of **2** in CH_2Cl_2 (20 mL) was bubbled with CO at −76 °C for 3 min. To this solution was added an aliquot of $\mathbf{H^+B^-}$ (0.21 g; 2.1×10^{-4} mol) in CH_2Cl_2 (5 mL) at −76 °C, and the solution was warmed to room temperature and stirred for 15 min. The solution was concentrated to ∼3 mL under vacuum, and hexanes were added to precipitate an oily residue (crude yield 95%). The hexanes were decanted, and ∼1 mL of CH_2Cl_2 was added to the oily residue. After 1 week under an atmosphere of hexanes vapor at 25 °C, light yellow crystals formed in the oily residue. The crystals were carefully collected, washed with hexanes, and dried under vacuum. Yield: 0.020 g; 7%. ^{1}H NMR (CD_2-Cl_2; 300 MHz; 293 K): δ 7.60−7.80 (m, 20 H, P*Ph*$_2$, B(3,5-C_6H_3(CF_3)$_2$)$_4$), 7.26 (m, 2 H, P*Ph*$_2$), 6.62 (t, J_{HH} = 6.3 Hz, 1 H, η^6-C_6H_5), 6.56 (t, J_{HH} = 6.3 Hz, 1 H, η^6-C_6H_5), 6.28, (d, J_{HH} = 6.3 Hz, 1 H, η^6-C_6H_5), 6.22 (t, J_{HH} = 6.3 Hz, 1 H, η^6-C_6H_5), 5.92 (d, J_{HH} = 6.3 Hz, 1 H, η^6-C_6H_5), 3.61 (m, 1 H, C_6H_5-CH_2CH_2P), 3.36 (m, 1 H, $C_6H_5CH_2CH_2P$), 2.90 (m, 1 H, $C_6H_5CH_2CH_2P$), 2.30 (m, 1 H, $C_6H_5CH_2CH_2P$), 0.29 (d, J_{HP} = 5 Hz, 3 H, Ru*CH*$_3$). ^{13}C NMR (CD_2Cl_2; 75.5 MHz; 293 K): δ 196.03, 162.38 (q, J_{CB} = 79.7 Hz), 135.44, 131.7−134.1 (m), 128.4−130.4 (m), 125.23 (q, $^1J_{CF}$ = 270.2 Hz), 118.09, 112.79, 102.47, 99.47, 93.20, 92.72, 48.94 (d, J_{CP} = 34.8 Hz), 30.35 (d, J_{CP} = 15.4 Hz), −16.76. IR (Nujol, cm^{-1}): 2004, 1276, 1124, 888, 842.

Synthesis of [(η^6:η^1-$C_6H_5CH_2CH_2PCy_2$)Ru(η^3-CH_3CH-C_5H_5)][B(3,5-$C_6H_3(CF_3)_2)_4$] (5). A solution of 0.10 g (2.3×10^{-4} mol) of **1** in CH_2Cl_2 (20 mL) was bubbled with acetylene at −76 °C for 3 min. To this solution was added an aliquot of $\mathbf{H^+B^-}$ (0.21 g; 2.1×10^{-4} mol) in CH_2Cl_2 (5 mL) at −76 °C, and the solution was warmed to room temperature and stirred for 90 min. The polyacetylene[44] was collected by filtration. The volatiles were removed from the filtrate under vacuum. The resultant reddish brown residue was washed with hexanes and extracted with benzene. The solution was filtered, and the benzene was evaporated under vacuum. The product was recrystallized from a mixture of CH_2Cl_2 and hexanes to afford 0.173 g (52% yield) of red crystals of **5**. ^{1}H NMR (CD_2Cl_2; 300 MHz; 293 K): δ 7.71 (s, 8 H, B(3,5-C_6H_3(CF_3)$_2$)$_4$), 7.55 (s, 4 H, B(3,5-C_6H_3(CF_3)$_2$)$_4$), 6.60 (m, 1 H, -*CH*=CH−), 6.26 (m, 1 H, −CH=*CH*−), 5.93 (d, J_{HH} = 5.7 Hz, 1 H, η^6-C_6H_5), 5.79 (d, J_{HH} = 5.7 Hz, 1 H, η^6-C_6H_5), 5.50 (t, J_{HH} = 5.7 Hz, 1 H, η^6-C_6H_5), 5.12 (t, J_{HH} = 5.7 Hz, 1 H, η^6-C_6H_5), 3.94 (t, J_{HH} = 5.7 Hz, 1 H, η^6-C_6H_5), 3.86 (d, J_{HH} = 10.5 Hz, 1 H, η^3-CH_3CHCCH), 3.26 (m, 1 H, η^3-CH_3CHCCH), 3.02 (m, 2 H, CCH_2CH), 2.69 (m, 2 H, $C_6H_5CH_2CH_2P$), 2.51 (m, 1 H, $C_6H_5CH_2CH_2P$), 2.35 (m, 1 H, $C_6H_5CH_2CH_2P$), 1.95 (d, J_{HH} = 6.3 Hz, 3 H, *CH*$_3$CHC=CH), 1.91 (m, 5 H, *Cy*$_2$), 1.80 (m, 6 H, *Cy*$_2$) 1.27 (m, 11 H, *Cy*$_2$). ^{13}C NMR (CD_2Cl_2; 75.5 MHz; 293 K): δ 162.38 (q, J_{CB} = 79.7 Hz), 139.32, 135.44, 129.61, 129.34 (q, $^2J_{CF}$ = 33.0 Hz), 125.24 (q, $^1J_{CF}$ = 272.1 Hz), 118.13, 114.65, 111.66, 99.25, 94.43, 92.73 (d, J = 7.2 Hz), 84.43, 84.17, 64.53, 52.53, 40.28, 37.72 (d, J_{CP} = 26 Hz), 35.43 (d, J_{CP} = 19.6 Hz), 34.50 (d, J = 20.2 Hz), 31.58, 29.48, 28.98, 28.11, 27.98, 27.89, 27.73, 27.35, 27.23, 26.62, 20.11.

Synthesis of [(η^6:η^1-$C_6H_5CH_2CH_2PPh_2$)Ru(η^3-CH_3CH-C_5H_5)][B(3,5-$C_6H_3(CF_3)_2)_4$] (6). This compound was prepared using a procedure analogous to that used to prepare **5**. Yield: 0.159 g; 52% of red crystals. ^{1}H NMR (CD_2Cl_2; 300 MHz; 293 K): δ 7.25−7.74 (m, 22 H, P*Ph*$_2$, B(3,5-C_6H_3(CF_3)$_2$)$_4$), 6.60 (m, −*CH*=CH−), 6.26 (m, 1 H −CH=*CH*−), 6.12 (d, J_{HH} = 6.0 Hz, 1 H, η^6-C_6H_5), 5.91, (d, J_{HH} = 6.0 Hz, 1 H, η^6-C_6H_5), 5.81 (t, J_{HH} = 6.0 Hz, 1 H, η^6-C_6H_5), 5.28 (t, J_{HH} = 6.0 Hz, 1 H, η^6-C_6H_5), 4.20 (t, J_{HH} = 6.0 Hz, 1 H, η^6-C_6H_5), 3.32 (m, 2 H, C_6H_5-CH_2CH_2P), 3.05 (br s, 3 H, CCH_2CH, η^3−CH_3CHCCH), 2.54 (m, 1 H, η^3-CH_3CHCCH), 2.43 (m, 2 H, $C_6H_5CH_2CH_2P$), 1.96 (d, J_{HH} = 6.0 Hz, 3 H, η^3-CH_3CHCCH). ^{13}C NMR (CD_2Cl_2; 75.5 MHz; 293 K): δ 162.38 (q, J_{CB} = 79.7 Hz), 139.03, 134.73, 132.4−133.5 (m), 129.2 (m), 124.72 (q, $^1J_{CF}$ = 272.6 Hz), 117.40, 114.91, 111.87, 101.81, 96.81 (d, J_{CP} = 2.1 Hz), 91.68 (d, J_{CP} = 9.7 Hz), 86.57, 85.48, 69.34, 58.65, 47.53 (d, J_{CP} = 33.4 Hz), 40.86, 28.26 (d, J_{CP} = 3.9 Hz), 20.45.

Synthesis of the Metastable Precursor to 7: [(η^6:η^1-$C_6H_5CH_2CH_2PPh_2$)RuCH$_3$(CH_2=CH_2)][B(3,5-C_6H_3-$(CF_3)_2)_4$]. A solution of 15 mg (3.6×10^{-5} mol) of **1** in CD_2Cl_2 (0.5 mL) was bubbled with ethylene at −76 °C for 3 min. To this solution was added an aliquot of $\mathbf{H^+B^-}$ (32 mg; 3.2×10^{-5} mol) in CD_2Cl_2 (0.5 mL) at −76 °C, and the solution was warmed to room temperature and stirred for 5 min. The solvents were removed under vacuum. ^{1}H NMR (CD_2Cl_2; 300 MHz; 293 K): δ 7.22−7.74 (m, 22 H, P*Ph*$_2$, B(3,5-C_6H_3(CF_3)$_2$)$_4$), 6.35 (m, 2 H, η^6-C_6H_5), 6.28 (t, J_{HH} = 5.7 Hz, 1 H, η^6-C_6H_5), 5.78 (d, J_{HH} = 5.7 Hz, 1 H, η^6-C_6H_5), 5.61 (t, J_{HH} = 5.7 Hz, 1 H, η^6-C_6H_5), 3.40 (m, 2 H, CH_2=CH_2), 3.18 (m, 2 H, C_6H_5-CH_2CH_2P), 2.69 (m, 2 H, $C_6H_5CH_2CH_2P$), 2.03 (m, 2 H, CH_2=CH_2), −0.53 (d, J_{HP} = 7.8 Hz, 3 H, Ru*CH*$_3$).

Synthesis of [(η^6:η^1-$C_6H_5CH_2CH_2PPh_2$)RuCl]$_2$[B(3,5-$C_6H_3(CF_3)_2)_4$]$_2$ (7). A solution of 0.10 g (2.4×10^{-4} mol) of **2** in CH_2Cl_2 (20 mL) was bubbled with ethylene at −76 °C for 20 min. To this solution was added an aliquot of $\mathbf{H^+B^-}$ (0.21 g; 2.1×10^{-4} mol) in CH_2Cl_2 (5 mL) at −76 °C, and the solution was warmed to room temperature and stirred for 1.5 h under 1.2 atm of ethylene. The volatiles were removed under vacuum, and the resultant brownish yellow residue was washed with hexanes and extracted with benzene. The benzene was evaporated under vacuum. The crude product appeared to contain predominantly [(η^6:η^1-$C_6H_5CH_2CH_2PPh_2$)RuCH$_3$(CH_2=CH_2)]-[B(3,5-C_6H_3(CF_3)$_2$)$_4$] with some uncharacterized Ru−H side product, as judged by ^{1}H NMR spectroscopy. This crude product was dissolved in CH_2Cl_2 (20 mL), and the solution was stirred for 2 days at room temperature. The reaction mixture was concentrated to ∼3 mL under vacuum, and hexanes was added to precipitate large red needles of **7**. The crystals were collected by filtration and dried under vacuum. Yield: 0.16 g; 50%. ^{1}H NMR (CD_2Cl_2; 300 MHz; 293 K): δ 7.07−7.95 (m, 22 H, P*Ph*$_2$, B(3,5-C_6H_3(CF_3)$_2$)$_4$), 5.19 (t, 2 H, J_{HH} = 5.7 Hz, η^6-C_6H_5), 4.82 (t, J_{HH} = 5.7 Hz, 2 H, η^6-C_6H_5), 4.65 (d, J_{HH} = 5.7 Hz, 1 H, η^6-C_6H_5), 3.67 (m, 2 H, $C_6H_5CH_2CH_2P$), 2.48 (m, 2 H, $C_6H_5CH_2CH_2P$). ^{13}C NMR (CD_2Cl_2; 75.5 MHz; 293 K): δ 162.34 (q, J_{CB} = 79.7 Hz), 135.40, 133.4−134.7 (m), 127.9−130.0 (m), 124.51 (q, $^1J_{CF}$ = 272.4 Hz), 119.01, 118.09, 95.44, 90.99, 77.07, 48.02 (d, J_{CP} = 34.0 Hz), 27.52. A satisfactory analysis was not obtained, possibly due to contamination with the uncharacterized Ru−H side product described above. Anal. Calcd for $C_{104}H_{102}Ru_2P_2B_2F_{48}Cl_2$: C, 48.37; H, 3.95. Found: C, 45.94; H, 2.14.

Table 6. Crystal Data and Structure Refinement for 3

empirical formula	$C_{55}H_{49}BCl_2F_{24}O_{1.5}PRu$
fw	1403.69
temp	223(2) K
wavelength	0.710 73 Å
cryst syst	monoclinic
space group	$P2/n$
unit cell dimens	
a	15.6960(6) Å
b	21.9098(9) Å
c	17.5126(7) Å
α	90°
β	96.872(1)°
γ	90°
V	5979.3(4) Å^3
Z	4
density (calcd)	1.559 g/mL
abs coeff	0.492 mm^{-1}
F(000)	2820
cryst size	0.4 × 0.32 × 0.22 mm
θ range for data collecn	1.60−23.52°
limiting indices	$-17 < h < 17$, $0 < k < 24$, $0 < l < 19$
no. of rflns collected	27 662
no. of indep rflns	9125 ($R_{int} = 0.0233$)
abs cor	empirical
max and min transmissn	0.6951 and 0.6017
refinement method	full-matrix least squares on F^2
no. of data/restraints/params	8839/8/947
goodness of fit on F^2	1.022
final R indices ($I > 4\sigma(I)$)	R1 = 0.0495, wR2 = 0.1245
R indices (all data)	R1 = 0.0646, wR2 = 0.1401
largest diff peak and hole	0.772 and −0.774 e/Å^3

Table 7. Crystal Data and Structure Refinement for 5

empirical formula	$C_{60}H_{54}BF_{24}PRu$
fw	1444.78
temp	223(2) K
wavelength	0.710 73 Å
cryst syst	monoclinic
space group	$P2_1/n$
unit cell dimens	
a	12.9055(6) Å
b	26.6420(11) Å
c	17.9855(8) Å
α	90°
β	90.090(1)°
γ	90°
V	6183.9(5) Å^3
Z	4
density (calcd)	1.552 g/mL
abs coeff	0.477 mm^{-1}
F(000)	2912
cryst size	0.35 × 0.20 × 0.20 mm
θ range for data collecn	1.37−23.26°
limiting indices	$-14 < h < 14$, $0 < k < 29$, $0 < l < 19$
no. of rflns collected	28 055
no. of indep rflns	9105 ($R_{int} = 0.0282$)
abs cor	empirical
max and min transmissn	0.84253 and 0.76093
refinement method	full-matrix least squares on F^2
no. of data/restraints/params	8882/45/1075
goodness of fit on F^2	1.024
final R indices ($I > 4\sigma(I)$)	R1 = 0.0386, wR2 = 0.0918
R indices (all data)	R1 = 0.0557, wR2 = 0.1043
largest diff peak and hole	0.568 and −0.582 e/Å^3

Polymerization of Norbornene. All polymerizations were conducted under nitrogen in an inert-atmosphere box. An aliquot of norbornene (0.56 g, 6.0 × 10^{-3} mol) and the activator (5 μmol) were dissolved in 10 mL of CH_2Cl_2. To this solution was added 5 μmol of complex **1** or **2**. The mixture was stirred for 1 h at ambient temperature and then poured into 200 mL of ethanol. The precipitated polymer was dissolved in CH_2Cl_2 (10−20 mL) and reprecipitated into 200 mL of ethanol. The polymer was collected by filtration and dried under vacuum. Control experiments performed under identical conditions but excluding the Ru complexes afforded no polynorbornene.

Table 8. Crystal Data and Structure Refinement for 6

empirical formula	$C_{59}H_{40}BCl_2F_{24}PRu$
fw	1347.76
temp	223(2) K
wavelength	0.710 73 Å
cryst syst	monoclinic
space group	$P2_1/n$
unit cell dimens	
a	13.2999(7) Å
b	12.6649(7) Å
c	33.5125(18) Å
α	90°
β	93.193(1)°
γ	90°
V	5636.1(5) Å^3
Z	4
density (calcd)	1.588 g/mL
abs coeff	0.426 mm^{-1}
F(000)	2696
cryst size	0.30 × 0.25 × 0.20 mm
θ range for data collecn	1.22−23.27°
limiting indices	$-14 < h < 14$, $0 < k < 14$, $0 < l < 37$
no. of rflns collected	24 126
no. of indep rflns	8373 ($R_{int} = 0.0282$)
abs cor	empirical
max and min transmissn	0.8343 and 0.7457
refinement method	full matrix least-squares on F^2
no. of data/restraints/params	8021/30/943
goodness of fit on F^2	1.180
final R indices ($I > 4\sigma(I)$)	R1 = 0.0440, wR2 = 0.0897
R indices (all data)	R1 = 0.0847, wR2 = 0.1182
largest diff peak and hole	0.661 and −0.646 e/Å^3

Table 9. Crystal Data and Structure Refinement for 7

empirical formula	$C_{104}H_{62}P_2B_2Cl_2F_{48}Ru_2$
fw	2580.14
temp	223(2) K
wavelength	0.710 73 Å
cryst syst	triclinic
space group	$P\bar{1}$
unit cell dimens	
a	13.6447(7) Å
b	14.5977(7) Å
c	14.6268(7) Å
α	86.823(1)°
β	69.788(1)°
γ	90°
V	2611.4(2) Å^3
Z	1
density (calcd)	1.641 g/mL
abs coeff	0.505 mm^{-1}
F(000)	1280
cryst size	0.40 × 0.35 × 0.30 mm
θ range for data collecn	1.81−23.55°
limiting indices	$-14 < h < 15$, $-16 < k < 16$, $0 < l < 16$
no. of rflns collected	12 064
no. of indep rflns	7665 ($R_{int} = 0.0282$)
abs cor	empirical
max and min transmissn	0.74066 and 0.69678
refinement method	full-matrix least squares on F^2
no. of data/restraints/params	7661/8/757
goodness of fit on F^2	1.022
final R indices ($I > 4\sigma(I)$)	R1 = 0.0467, wR2 = 0.1072
R indices (all data)	R1 = 0.0525, wR2 = 0.1124
largest diff peak and hole	0.959 and −0.970 e/Å^3

Molecular Weight Determinations. Molecular weights of the polymers were determined by gel permeation chromatography (GPC) performed using a Waters GPC system equipped with two Waters Styragel HR columns and a 410

differential refractometer. Tetrahydrofuran (THF) was used as the eluant at a flow rate of 1.0 mL/min. Molecular weights were calculated from a calibration curve of narrow molecular weight polystyrene standards purchased from Polysciences. GPC samples (3−5 mg/mL) were filtered through a 0.5 μm filter prior to injection into the chromatograph.

X-ray Crystal Structure Determinations. The crystallographic data collection parameters for each compound are summarized in Tables 6−9. All measurements were made with a Siemens SMART platform diffractometer equipped with a 1K CCD area detector. A hemisphere of data (1271 frames at 5 cm detector distance) was collected using a narrow-frame method with scan widths of 0.30% in ω and an exposure time of 25 s/frame. The first 50 frames were remeasured at the end of data collection to monitor instrument and crystal stability, and the maximum correction on I was <1%. The data were integrated using the Siemens SAINT program, with the intensities corrected for Lorentz factor, polarization, air absorption, and absorption due to variation in the path length through the detector faceplate. A ψ scan absorption correction was applied on the basis of the entire data set. Redundant reflections were averaged. All of the CF_3 groups were found to be seriously disordered, with most of them having three distinct orientations. The disorder was treated by introducing ideal rigid-body models at each site and refining the occupancy factors, while keeping the total occupancy in each group at 100%. In the final cycles of refinement, those CF_3 groups having occupancies greater than 30−35% were refined anisotropically.

In compound **3**, the C17−C22 cyclohexyl ring was also found to be slightly disordered over two positions, and the methylene chloride solvent was massively disordered over at least four different orientations. Additionally, a single site of remaining electron density was located apart from all of the other molecular species. This site was refined as oxygen and is presumed to be an interstitial molecule of water present about half of the time, as reflected in the reported empirical formula (Table 6). In compound **5**, the vinyl ligand was disordered approximately 50:50 about a pseudo-mirror and failed to refine well due to high correlations. Therefore, distance constraints were used on the basis of the geometry found in the ordered analogue **6**. Weighted R factors (R_w) and all goodness of fit (S) values are based on F^2; conventional R factors (R) are based on F.

Acknowledgment. The Robert A. Welch Foundation (Grant E-1320) and the National Science Foundation (CAREER Award to T.R.L., Grant No. CHE-9625003) provided generous support for this research. We thank Dr. James Korp for technical assistance with the X-ray crystallographic analyses. We also thank Professors Thomas Albright and David Hoffman for many helpful discussions.

Supporting Information Available: Tables giving X-ray crystallographic data for complexes **3** and **5**−**7** and figures giving ^{1}H NMR spectra of complexes **4**−**7**. This information is available free of charge via the Internet at http://pubs.acs.org.

OM030008S